Molluscum Contagiosum Virus protein MC005 inhibits NFκB activation by targeting NEMO-regulated IKK activation

Gareth Brady[1,#*], Darya A. Haas[2], Paul J. Farrell[3], Andreas Pichlmair[2] and Andrew G. Bowie[1,#].

[1]School of Biochemistry and Immunology, Trinity Biomedical Sciences Institute, Trinity College Dublin, Dublin 2, Ireland. [2]Max Plank Institute of Biochemistry, Am Klopferspitz 18, 82152 Martinsried, Germany. [3]Section of Virology, Imperial College Faculty of Medicine, Norfolk Place, London W2 1PG, UK

Running Head: Inhibition of NFκB by poxvirus MCV protein MC005

*Present address: Trinity Translational Medicine Institute, Department of Clinical Medicine, School of Medicine, Trinity College Dublin, Dublin 8, Ireland

[#]Address correspondence to Gareth Brady, bradyg1@tcd.ie or Andrew G. Bowie, agbowie@tcd.ie

Abstract word count: 249

Text word count: 9432

Abstract

Molluscum Contagiosum Virus (MCV), the only known extant, human-adapted poxvirus, causes a long-duration infection characterized by skin lesions that typically display an absence of inflammation despite containing high titres of live virus. Despite this curious presentation, MCV is very poorly characterized in terms of host-pathogen interactions. The absence of inflammation around MCV lesions suggests the presence of potent inhibitors of human anti-viral immunity and inflammation. However, only a small number of MCV immunomodulatory genes have been characterized in detail. It is likely that many more remain to be discovered given the density of such sequences in other poxviral genomes. NFκB activation occurs in response to both virus-induced pattern recognition receptor (PRR) signaling and cellular activation by virus-induced pro-inflammatory cytokines like TNF and IL-1. Activated NFκB drives cytokine and interferon gene expression leading to inflammation and virus clearance. We report that MC005, which has no orthologs in other poxviral genomes, is a novel inhibitor of PRR- and cytokine-stimulated NFκB activation. MC005 inhibited NFκB proximal to the IκB kinase (IKK) complex, and unbiased affinity purification revealed that MC005 interacts with the IKK subunit NEMO. MC005 binding to NEMO prevents conformational priming of the IKK complex that occurs when NEMO binds to ubiquitin chains during pathway activation. This data reveals a novel mechanism for poxviral inhibition of human innate immunity, validates current dynamic models for NEMO-dependent IKK complex activation and further clarifies how the human-adapted poxvirus MCV can so effectively evade anti-viral immunity and suppress inflammation to persist in human skin lesions.

Importance

Poxviruses adapt to specific hosts over time evolving and tailoring elegantly precise inhibitors of the rate-limiting steps within the signaling pathways that control innate immunity and inflammation. These inhibitors reveal new features of the anti-viral response, clarify existing models of signaling regulation while offering potent new tools for approaching therapeutic intervention in autoimmunity and inflammatory disease. Molluscum Contagiosum Virus (MCV) is the only known extant poxvirus specifically adapted to human infection and appears adept at evading normal human anti-viral responses yet it remains poorly characterized. We report the identification of MCV protein MC005 as an inhibitor of the pathways leading to activation of NFκB, an essential regulator of innate immunity. Further, identification of the mechanism of inhibition of NFκB by MC005 confirms current models of the complex way in which NFκB is regulated and greatly expands our understanding of how MCV so effectively evades human immunity.

Introduction

Host innate immune detection of virus infection employs pattern recognition receptors (PRRs) such as Toll-like receptors (TLRs) and cytosolic nucleic acid-sensing systems, which stimulate signal transduction cascades leading to the activation of NFκB (nuclear factor kappa-light-chain-enhancer of activated B cells) and IRF (interferon regulatory factor) transcription factor families. Such transcription factors induce type I interferons (IFNs) and the pro-inflammatory cytokines tumor necrosis factor α (TNFα) and interleukin-1 (IL-1) (1). IFNs and cytokines then stimulate pathways which limit viral spread and direct anti-viral acquired immunity. In order to overcome these host defense mechanisms, viruses evolve inhibitors that target the key, rate-limiting steps in innate immune signaling. Thus, studying such inhibitors not only provides an understanding of viral pathogenesis but also reveals novel facets of the host innate signaling mechanisms which the inhibitors target, in addition to validating existing models describing the complexity of pathway activation. This provides avenues for therapeutic intervention in disorders defined by aberrant innate responses and inflammation. This is particularly true of poxviruses, which have evolved small inhibitory proteins by integrating host sequences into their genomes. These proteins then further evolve by refinement of their inhibitory activity through gradual mutation over long periods of virus-host evolution (2). Although the discovery and characterization of such poxviral inhibitory proteins in non-human adapted poxviruses like vaccinia virus (VACV) has been highly informative in defining host-virus interactions and uncovering novel aspects of innate immunity (3), only a small number of these inhibitors have been described for the only known extant human-adapted poxvirus Molluscum Contagiosum Virus (MCV).

MCV is specifically adapted to human infection and has a genome predicted to encode 182 proteins, only 105 of which have orthologs in other orthopoxviruses (4). In contrast to the non-human adapted VACV, which causes local inflammation in human skin

lesions, MCV can inhabit human dermal lesions over long periods of time with minimal evident immune response and almost no inflammation, despite producing what are likely to be highly antigenic proteins. While this predicts that MCV has evolved unique, efficient inhibitors of human innate immunity, less than ten MCV immunoregulators have been investigated in detail (5-7). Hence, we screened a library of open reading frames (ORFs) with no known function from the MCV genome for inhibition of human anti-viral innate immune signaling networks that culminate in the activation of NFκB, a critical pro-inflammatory transcription factor. This identified MC005, a protein with no orthologs in other poxviral genomes, as a novel inhibitor of NFκB activation. MC005 was previously shown to be expressed as an early gene product in MCV infection consistent with a role in immunoregulation (8). Here we show that MC005 inhibited NFκB activation stimulated by pro-inflammatory cytokines, PRR ligands and DNA virus or RNA virus infection. Further functional analysis including unbiased affinity purification to identify host targets of MC005 showed that MC005 binds the IκB kinase (IKK) complex through the regulatory subunit IKKγ/NEMO. MC005 binds to NEMO (NF-kappa-B essential modulator) in a specific region between the ubiquitin-binding UBAN (Ubiquitin binding in ABIN and NEMO) domain and the region where NEMO binds the IKK subunits. As the current model of IKK activation suggests that ubiquitin binding causes a conformational change within the UBAN domain which conducts a change to the IKKs bound upstream thereby priming them for activation, we propose that MC005 inhibits this conformational conduction of the priming signal thus inhibiting IKK activation and thus downstream NFκB activation. These discoveries not only validate the model of IKK regulation but also greatly extend our understanding of how MCV, the only known extant human-adapted poxvirus, so efficiently evades human immunity.

Materials and Methods

Cell Culture and viruses

Human embryonic kidney 293T (HEK293T) cells, HeLa and COS-1 cells were maintained in Dulbecco's Modified Eagle's Medium (DMEM) containing 10% (v/v) FCS and penicillin-streptomycin. THP1 cells were maintained in RPMI medium containing 10% (v/v) FCS and penicillin-streptomycin. Lentiviral stable cells were maintained in or selected with 5 μg/ml puromycin, pCEP4 and pMEP4-Stable cells were selected with 300μg/ml Hygrogold (Invivogen) and expression of MC005 induced in pMEP4 lines with 1μM cadmium chloride (Sigma). Sendai Virus (ECACC), Vesicular Stomatitis virus (a gift from John C. Bell, Ottawa Hospital Research Institute) and Modified Vaccinia Ankara (a gift from Ingo Drexler, Düsseldorf University) were all used at an MOI of 10.

Plasmids and oligonucleotides.

MC005 was custom synthesized by Genscript and sub-cloned into K*pn*I and N*ot*I sites of pCEP and cadmium chloride-inducible pMEP4 plasmids (Invitrogen) with a C-terminal FLAG tag (DYKDDDDK) or HA tag (YPYDVPDYA). pCEP4-MC014-FLAG was described previously (7). The primer sets for cloning of full-length and truncated MC005 into pCEP4 corresponded to 18 bp of indicated sequence with K*pn*I and H*ind*III overhanging restriction sites for insertion into the construct in these sites upstream of a FLAG tag. NEMO truncations were made with primers corresponding to 18bps indicated 5' and 3' regions flanked by K*pn*I and H*ind*III overhanging restriction sites for insertion into pCEP4 in these sites upstream of a HA tag sequence. pdI-MC005, the retroviral expression construct used the direct 5' and 3' sequences of MC005L with SpeI and MluI overhangs respectively with a C-terminal FLAG tag. Plasmids expressing FLAG -IKKβ, FLAG -TAB2, FLAG -TRAF2 and FLAG -TRAF6 were from Tularik Inc. The sources of other expression plasmids were as follows: FLAG -TRIF (S. Akira, Osaka University, Osaka, Japan), Myc-MyD88 (L. O'Neill, Trinity College Dublin, Ireland), CD4-TLR9 (A. Ozinsky, University of Washington, WA),

CD4-TLR3 (R. Medzhitov (Yale University, CT), FLAG-MAVS and cGAS (J. Chen, UT Southwestern Medical Centre), RasVHa (D. Cantrell, University of Dundee, Dundee, UK), human STING coding region was amplified by PCR from full-length I.M.A.G.E. cDNA clones (IRATp970D0274D and IRAVp968F0688D; imaGenes) and were cloned into the vector pCMV-myc (Clontech)), HA-Ubiquitin (A. Mansell, Monash University, Melbourne, Australia). The NFκB-luciferase reporter gene was from R. Hofmeister (Universitat Regensburg, Germany), the ISRE-luciferase was from L. O'Neill, while the pFR-luciferase reporter and pFA2-Elk1 were from Agilent. Full-length NEMO- FLAG and NEMO-HA (K. Fitzgerald, UMASS, US). The NEMO K277A mutant was generated performing site-directed mutagenesis on the region using the primers: FP: aggaggc cctggtggccgcacaggaggtgatcgataagctg, RP: cagcttatcgatcacctcctgtgcggccaccag ggcctcct.

Antibodies

Primary Abs used for immunoblotting were anti–β-actin (AC-74) and anti- FLAG (M2) from Sigma-Aldrich, anti-IκBα (R. Hay, University of Dundee, Dundee, U.K.), anti–phospho-p65 (Ser536, 93H1), anti-p65 (C-20, Santa Cruz), phospho-IKKα/β (Ser176/180) (16A6) Rabbit mAb (CST) and anti-HA (Covance). The secondary Abs for immunoblotting were IRDye 680LT anti-mouse, IRDye 800CW anti-rabbit, and IRDye 680LT anti-goat (LI-COR Biosciences). Secondary Abs for confocal microscopy were Alexa Fluor 647 anti-mouse or Alexa Fluor 488 anti-rabbit (Invitrogen).

ELISA

Cell culture supernatants were assayed for IL8 and IP-10 protein using an ELISA kit (R&D Systems) according to the manufacturer's instructions.

Immunoblotting

Cells were seeded at 5 x 10^5 cells/well in 6-well dishes and transfected with 3µg total DNA using GeneJuice (Novagen) the next day. 24 h later cells were lysed in 200µl sample buffer

(187.5 mM Tris [pH 6.8], 6% [w/v] SDS, 30% [v/v] glycerol, 0.3% [w/v] bromophenol blue, 150 mM DTT and benzonase), incubated on ice for 5 minutes and then boiled for 5 min at 99°C. 20 µl lysates were resolved on 10-20% SDS-PAGE, transferred to polyvinylidene difluoride membrane (Millipore), blocked for 1 h in 3% (w/v) BSA in PBS, and probed overnight with primary Ab (1:1000 dilution in blocking solution). The next day, membranes were incubated with secondary Abs (1:10,000 dilution in blocking solution) and blots were visualized using the Odyssey imaging system (LI-COR Biosciences).

Immunoprecipitation

Cells were seeded at 4 x 10^6 cells/10cm dish and transfected with 8µg total plasmid the next day. Twenty-four hours later, cells were washed with ice-cold PBS, and then scraped into lysis buffer (50 mM Tris [pH 7.4], 150 mM NaCl, 0.5% [v/v] NP-40, 30 mM NaF, 5 mM EDTA, 10% [v/v] glycerol, 40 mM β-glycerophosphate, containing the inhibitors 1 mM Na_3VO4, 1 mM PMSF, and 1% [v/v] aprotinin) and left on ice for 45 min. Anti- FLAG beads (Sigma) were equilibrated with lysis buffer and cleared lysates were mixed with beads and incubated for 2 hours rolling at 4ºC. Beads were then washed three times with 1ml lysis buffer and immunoprecipitated material was eluted with 3x FLAG peptide (Sigma) for 30 minutes rolling at 4ºC after which it was separated and immunoblotted for indicated proteins.

Confocal microscopy

Cells were seeded at 3 x 10^5 cells/ml on glass coverslips in 24-well plates and stimulated the next day as indicated. Cells were fixed for 12 min in 4% (w/v) paraformaldehyde and permeabilized for 15 min with 0.5% (v/v) Triton X-100 in PBS. Coverslips were blocked for 1 h in 5% (w/v) BSA/ 0.05% (v/v) Tween 20 in PBS and stained overnight with primary Abs (1:200 dilution in blocking solution). The following day, coverslips were incubated for 3 h with secondary Abs (1:500 dilution in blocking solution) and mounted in Mowiol 4-88

(Calbiochem) containing 1 mg/ml DAPI. Images were obtained with an Olympus FV1000 confocal microscope using a 360x oil-immersion objective.

Reporter gene assays

For reporter gene assays, cells were seeded at 1 x 10^5 cells/ml in 96-well plates and transfected 16 h later using GeneJuice transfection reagent (Novagen) with 80 ng luciferase reporter gene, 20 ng pGL3-Renilla luciferase, indicated amounts of expression vectors and MCV ORFs, and adjusted to 230 ng total DNA with empty vector pCMV-HA. 24 h after transfection, cells were either stimulated with cytokines, infected with virus for 24 hours or directly lysed in passive lysis buffer (Promega) and analyzed for luciferase activity. Firefly luciferase activity was normalized to Renilla luciferase activity to control for transfection efficiency. For the Ras-driven Elk1 reporter assay, 1 ng of the pFA-Elk1 expression vector together with the pFR-luciferase reporter plasmid (80ng) were employed, using a RasVHa expression vector for pathway activation.

Generation of retroviral stable cell lines

Retroviral stable cell generation employed the pdlNotInPkMCSR expression construct (9), cloning into the M*lu*I and S*pe*I sites. Lentivirus was packaged using the *Virapower* packaging system (Invitrogen) following standard protocol as described in the manual. Stable cells were selected with 5 μg/ml puromycin.

Affinity purification and LC-MS/MS analysis

Expression of FLAG-tagged MC005 was induced with 1 μM $CdCl_2$ in stably transfected HEK293T cells. After 24 hours, cells were washed in 1x PBS, pelleted at 3000 x *g* for 5 min at 4°C, and snap-frozen in liquid nitrogen. Cell pellets were thawed on ice and resuspended in 1 ml ice-cold TAP lysis buffer (50 mM Tris-HCl pH 7.5, 4.3% glycerol, 0.2% NP-40, 1.5 mM MgCl2, 100 mM NaCl) supplemented with EDTA-free complete protease inhibitor cocktail (Roche) and 250 U benzonase (Sigma-Aldrich). After incubation on ice for 30 min,

lysates were centrifuged at 12000 x g for 5 min at 4°C. Cleared lysates were incubated with 40 µl anti-FLAG M2 affinity gel (Sigma-Aldrich) for one hour on a rotating wheel at 4°C. After incubation, resin was washed in TAP lysis buffer (final 2 washes without NP-40) and resuspended in 40 µl 6 M guanidinium-HCl in 100 mM Tris pH 8.5 supplemented with 10 mM TCEP and 40 mM chloroacetamide. After 30 min incubation at RT in the dark, lysates were diluted 1:10 with digestion buffer (10% acetonitrile, 25 mM Tris pH 8.5) and incubated with 0.5 µg EndoLysC (Wako Chemicals) and 0.5 µg sequencing grade modified trypsin (Promega) overnight on a rotating wheel at RT. After digestion, peptides were acidified with trifluoracetic acid, desalted on reversed phase C18 StageTips, and eluted before LC-MS/MS using buffer B (80% acetonitrile, 0.5% acetic acid). Eluted peptides were analyzed on a nanoflow EASY-nLC system coupled to LTQ-Orbitrap XL mass spectrometer (Thermo Fisher Scientific). Peptide separation was achieved on a C18-reversed phase column (ReproSil-Pur C18-AQ, 1.9 µm, 200x0.075 mm, Dr. Maisch) using a 120-min linear gradient from 2 to 60% acetonitrile in 0.1% formic acid. LTQ-Orbitrap XL was operated with a Top10 MS/MS spectra acquisition method in the linear ion trap per MS full scan in the orbitrap. Raw files were processed with MaxQuant (version 1.4.1.4) and searched with built-in Andromeda search engine against a human protein database (UniprotKB, release 2012_01) concatenated with a decoy of reversed sequences, using label-free quantification (LFQ) algorithm as described previously (10). Carbamidomethylation was set as fixed modification while methionine oxidation and protein N-acetylation were included as variable modifications. The search was performed with an initial mass tolerance of 6 ppm for the precursor ion and 0.5 Da for the fragment ions. Search results were filtered in Perseus (version 1.4.1.8) with a false discovery rate (FDR) of 0.01. Prior to statistical analysis, known contaminants and reverse hits were removed. Proteins identified with at least 2 unique peptides and a minimum of 2 quantitation events in at least one experimental group were

considered for analysis. LFQ protein intensity values were log-transformed and missing values were filled in by imputation with random numbers drawn from a normal distribution. Significant interactors were determined using two-sample *t* test with welch correction after 250 permutations and FDR threshold set to 0.01, and S_0 empirically set to 1. Results were plotted using R (release version 2.15.3).

Results

Identification of a MC005 as a novel MCV inhibitor of PRR-driven NFκB activation.

In order to identify novel MCV inhibitors of human innate anti-viral sensing, we analyzed the MCV genome for ORFs predicted to encode small, soluble proteins of unknown function, and tested the effect of expression of a library of MCV ORFs on viral nucleic acid signaling, the first innate stimulus that occurs during viral infection and leads to the production of pro-inflammatory cytokine, chemokine and type I interferon production (3). Initial screening identified MC005 as a potential inhibitor of nucleic acid signaling (data not shown). Due to the presence of a robust, well-characterised, endogenous nucleic acid sensing PRR system in the THP-1 human monocytic cell line, we generated stable MCV protein-expressing lines by lentiviral transduction and stable selection. Control empty vector and MC005-expressing stable cell lines were then stimulated by transfection with poly(dA:dT) dsDNA prior to measurement of the production of IP-10 (CXCL10), an NFκB-and IRF-dependent, PRR-inducible chemokine produced during poxvirus infection (11-13). Stable MC005 expression was detected (Fig. 1A) and this was correlated with a significant decrease in poly(dA:dT)-induced IP-10 was observed in the presence of this viral protein (Fig. 1B). RNA virus-induced IP-10 production was also significantly inhibited by MC005 (Fig. 1C).

In order to determine whether inhibition by MC005 was at the level of promoter induction, we next examined the effect of MC005 on the activity of the IFNβ promoter,

which like IP-10 is NFκB-and IRF-dependent, by luciferase reporter gene assay. As an in vitro infection model for MCV is not currently available, we examined the effect of MC005 expression on the activity of the IFNβ promoter induced by infection of HEK293T cells with the distantly related poxvirus modified vaccinia Ankara (MVA). MC005 is a 9kD protein and when expressed in HEK293T cells localizes throughout the cells (Fig. 1D). Fig. 1E shows a significant and dose-dependent inhibition of IFNβ promoter activation by MC005 but not by MC014, an irrelevant MCV protein that was expressed at similar levels to MC005 (Fig. 1F). A similar dose-dependent inhibition of the IFNβ promoter activation by MC005 was seen after Sendai virus infection of these cells (Fig. 1G).

As virus- and PRR-induced IFNβ and IP-10 induction occurs through both NFκB-and IRF family transcription factor activation, we next examined the effect of MC005 on the activation of these transcription factors. After entry into cells and uncoating, sensing of poxvirus during infection can occur through DNA genome sensing by cGAMP synthase (cGAS) cytosolic DNA sensor which then signals to transcription factors via STING (14, 15). Co-expression of cGAS and STING in HEK293T cells, which don't normally contain these proteins, reconstitutes cGAS-STING signaling (7, 16), leading to both NFκB and IRF activation. Interestingly, while MC005 had no significant effect on cGAS-induced IRF activation (measured by ISRE promoter-driven luciferase expression), cGAS-induced NFκB activation (measured by κB promoter-driven luciferase expression) was inhibited (Fig. 1H and 1I).

In HEK293T cells, RNA Polymerase III transcribes AT-rich DNA such as poly(dA:dT) into an RNA ligand that activates the RIG-I/MAVS sensing system and this system has been implicated in sensing intracellular poxviral DNA (17). Poly(dA:dT) stimulation of NFκB activation was also inhibited by MC005 as was NFκB activation with MAVS (Fig. 1J and 1K). We next examined the effect of MC005 on virus-induced NFκB

activation and found that MC005 also inhibited activation of this transcription factor by infection with either the RNA virus Vesicular Stomatitis Virus (VSV) or poxvirus MVA (Fig. 1L and 1M).

TLR3 and TLR9 have been shown to play key roles in sensing poxvirus infection *in vivo* (18, 19) and both are characteristically upregulated in MCV-infected lesions despite a lack of inflammation or viral clearance in such lesions in most circumstances (20). We next examined the effect of MC005 expression on TLR9 and TLR3 signaling using constitutively active CD4 fusions of these PRRs. Similar to the other PRR systems investigated, MC005 inhibited NFκB activation but not IRF activation by these pathways (Fig. 2 A-D). Additionally, activation of the TLR3 pathway further downstream by expressing its adapter TRIF activated both NFκB and IRFs and as for the other stimuli MC005 inhibited NFκB but not IRF activity (Fig. 2E and F) suggesting that the point of inhibition lay further downstream. Together, these data suggested that MC005 targeted PRR-stimulated NFκB but not IRF, activity.

MC005 inhibits NFκB activation stimulated by the pro-inflammatory cytokines TNF and IL-1.

In addition to type I IFNs, primary virus sensing through PRRs leads to the upregulation and secretion of pro-inflammatory cytokines which directly drive inflammation in infected tissue in order to create the conditions necessary for an adaptive immune response to occur leading to virus clearance. Such inflammation is absent for extended periods during MCV infection. Having demonstrated that MC005 inhibits NFκB but not IRF signaling by PRRs, we next examined whether MC005 would also suppress pro-inflammatory cytokine-induced NFκB activity. Similar to PRR-driven NFκB activation, we observed that TNF-activated NFκB was also inhibited by MC005, but not by MC014 at equivalent levels of

expression (Fig. 3A and B). The specific effect of MC005 on NFκB activation was further suggested by the lack of effect on an unrelated mitogenic signaling pathway activated by a constitutively active form of Ras, RasVHa (21) (Fig. 3C). There, RasVHa activation of Elk1 is monitored using an Elk-1/GAL4 DNA-binding domain fusion which induces a GAL4 promoter luciferase system.

We next examined the effect of MC005 on the activation of NFκB by expression of TRAF2, a key regulatory component of the TNF receptor signaling pathway. MC005 inhibited NFκB by TRAF2 in three different cell lines: HEK293T (Fig. 3D), Cos-1 (Fig. 3E) and HeLa cells (Fig. 3F), demonstrating that MC005 inhibition was independent of cell type. We next established a MC005-expressing HEK293T stable cell line in order to investigate the effect of MC005 expression on TNFα-driven cytokine production. Using empty vector and MC005-expressing stable cells (Fig. 3G), we demonstrated that NFκB inhibition by MC005 translated into suppression of secretion of IL-8, an important NFκB-dependent chemokine produced during inflammation. (Fig. 3H).

In addition to TNFα, IL-1β plays a key role in local and systemic, virus-induced inflammation and both production and activity of this cytokine is heavily targeted by poxviruses (3). As with other stimuli, MC005 but not MC014 inhibited the activation of NFκB by IL-1 at similar levels of expression (Fig. 3I and 3J). MC005 also inhibited NFκB activation by TRAF6, a key component of the IL1 signaling pathway (Fig. 3K).

MC005 inhibits NFκB activation at the level of the IKK complex

Having demonstrated thus far that MC005 can inhibit both PRR sensing and pro-inflammatory cytokine stimulated activation of NFκB, we suspected that this viral inhibitor was targeting a point in signaling common to both sets of pathways. PRR- and pro-inflammatory cytokine stimulated NFκB activation is catalyzed by the activation of RING-

334 domain containing TRAF proteins like TRAF2 in the case of TNF and TRAF6 in the case of
335 both IL-1 and PRR signaling (Fig. 4A), which generate long chains of ubiquitin at activation
336 foci within cells. After generation of these ubiquitin chains, two complexes bind to the chains
337 in close proximity to each other, the TAB/TAK complex and the IKK complex. The IKK
338 complex is comprised of a regulatory ubiquitin binding protein NEMO (also known as IKKγ)
339 which regulates the activity of the active kinase subunits IKKα and IKKβ. Ubiquitin binding
340 by NEMO in the IKK complex, causes a conformational change in NEMO which primes
341 IKKβ for phosphorylation and activation by TAK1 (22, 23). Once active, IKKβ, for example,
342 then phosphorylates both the inhibitory protein IκBα (driving its proteasomal degradation)
343 and the p65 subunit of NFκB releasing the transcription factor to translocate to the nucleus
344 and induce anti-viral and pro-inflammatory gene expression.

345 The data presented thus far suggested that MC005 targets NFκB activation
346 downstream of TRAF2/6. Thus we next investigated the effect of MC005 expression on the
347 signaling events proximal to NFκB activation described above, in comparison to another
348 MCV protein, MC132, which we recently showed targets p65 for degradation (7).
349 Stimulating NFκB activation by the TAB/TAK complex (by overexpressing TAB2), we
350 observed that both MC005 and MC132 inhibited NFκB activation (Fig. 4B). In contrast to
351 this, stimulating NFκB activation by IKKβ (where overexpressing the kinase simulates
352 constitutive activation of the kinase without the normal regulation exerted on it by the IKK
353 complex in the absence of an upstream signal), bypassed the inhibitory activity of MC005,
354 but not of MC132 which targets p65 directly (Fig. 4C). A similar result was observed when
355 IKKα was expressed (data not shown). Consistent with MC005 inhibiting at the level of IKK
356 complex activation, we found that activating the NFκB-dependent reporter gene by
357 overexpressing p65 similarly bypassed the inhibitory activity of MC005 but not MC132 (Fig.

4D). These data thus suggested that MC005 was targeting NFκB activation at the level of the IKK complex.

MC005 interacts with NEMO

In order to gain insights into the mechanism by which MC005 was inhibiting at the level of the IKK complex, we investigated the cellular interactions of this viral protein by performing unbiased affinity purification combined with mass spectrometry (AP-MS). To do this, we generated a metallothionein promoter-inducible, MC005-expressing stable HEK293T cell line in which high levels of MC005- FLAG could be induced with $CdCl_2$ (Fig. 5A). Using this system we performed an analysis of MC005 cellular interaction partners by AP-MS. This showed that NEMO was the most significantly enriched protein in the MC005 immunoprecipitates (Fig. 5B).

We confirmed this interaction by expressing NEMO and MC005 and demonstrating that these proteins co-immunoprecipitated in both HEK293T cells (Fig. 5C) and Hela cells (Fig. 5D). We also demonstrated co-localisation of MC005 (predominantly localizing in the cytoplasm of Hela cells) with both NEMO and IKKβ by confocal microscopy (Fig. 5E). These data suggested that MC005 inhibited NFκB activation by binding NEMO within an intact IKK complex, downstream of TRAF activation. To confirm this, we investigated the association of MC005 with TRAF6. While a low level interaction with TRAF6 was evident, this interaction became significantly more pronounced when NEMO was overexpressed suggesting that NEMO is the specific interaction target of MC005 bridging an association with activated TRAF6 (Fig. 5F).

A central 46-amino acid motif is required for MC005 inhibition

To determine the region of MC005 required for inhibition of NFκB activation, we created a series of truncations of MC005 starting with the removal of large sections of the N and C terminus and then narrowing down the region required for inhibition with progressive deletion of both N and C-termini. Through this systematic approach we identified that the first 10 amino acids of the N-terminus and the last 29 amino acids of the C-terminus were dispensable for inhibitory activity, since only MC005 fragments containing residues 11-57 gave more than 50% NFκB inhibition (Fig. 6A and 6C). Interestingly, in most cases, the ability of an MC005 truncation to inhibit NFκB correlated with its ability to bind NEMO (Fig. 6B and 6C), further confirming this protein as the specific target through which MC005 inhibits NFκB activation.

MC005 prevents ubiquitin-binding dependent regulation of IKKβ activation by NEMO

While purified NEMO is dimeric in solution (24), cross-linking experiments indicate that the endogenous IKK complex is composed of four NEMO molecules and two molecules each of IKKα and IKKβ, consistent with its apparent molecular mass of 700-900kDa (25). This complex pre-exists prior to stimulation and the intact, endogenous, oligomeric complex is necessary for canonical NFκB activation (26). NEMO possesses a series of domains and regions which play key roles in complex assembly and in regulating IKK activation by bridging appropriate upstream signals to IKK activation. Thus NEMO is a central, regulatory cog in controlling the initiation of inflammation and a logical target for viral inhibition. Residues 1-80, which encompasses the N-terminus and half of the coiled coil (CC)-1 domain, have been shown to be vital for NEMO dimerization (Fig. 7A) (22). Residues 40-120 are where NEMO interacts with the IKKs, while residues 249-339, a region consisting of the CC2 and a Leucine Zipper (LZ) motif, comprise the UBAN domain which binds TRAF-regulated ubiquitin chains (Fig. 7A). The UBAN domain also regulates the conformational

change which occurs within NEMO that induces a 'priming' of IKKα and IKKβ for subsequent auto-phosphorylation and phosphorylation by TAK1.

To further characterise the mechanism by which MC005 was inhibiting the IKK complex by binding NEMO, we next investigated the region in NEMO to which MC005 was binding. To do this we generated a series of truncations of NEMO corresponding to the known functional domains and regions within this protein (Fig. 7A). While all the truncations of NEMO expressed to approximately equivalent levels (Fig. 7B), MC005 was able to interact with all of these truncations except one truncation lacking sequence N-terminal of the CC2 domain (directly between the IKK binding region and the UBAN domain) (Fig. 7B). Given that it effectively interacted with a truncation possessing the second half of the CC1 domain, this suggests that the viral protein is binding to a region between the second half of the CC2 domain and the beginning of the CC2 domain of NEMO.

We next examined the effect of MC005 on the regulatory events controlled by NEMO in inflammatory signaling and on IKK complex formation. We first investigated the effect of MC005 on the ubiquitination of NEMO and on its association with ubiquitin chains which is critical for its regulation and activation of the IKK complex at signaling foci within the cell. While we observed that expression of ubiquitin-HA induced both NEMO ubiquitination (indicated by a Ubiquitin-HA-dependent shift in the mass of NEMO- FLAG) and the association of this protein with ubiquitinated proteins, MC005 had no effect on these processes and interactions (Fig. 7C). To investigate whether the association of MC005 was disrupting the formation or assembly of the multimeric IKK complex, we next examined the effect of MC005 on the ability of NEMO to oligomerise with itself. This demonstrated that the NEMO-NEMO interaction was not affected by the presence of the viral protein (Fig. 7D). Additionally, the close co-localisation of MC005 with IKKβ (Fig. 5E) suggested that MC005

was not disrupting the association of the kinase subunits and thus was binding an intact IKK complex.

While heterologous expression of NEMO does not drive activation of the complex (as NEMO still requires ubiquitin chains from upstream activation events to mediate IKK activation), previous work demonstrated that a single mutation within the UBAN domain of murine NEMO simulates the conformational state that NEMO assumes after ubiquitin binding which primes IKKβ for phosphorylation by TAK1 (27). We generated the human equivalent site mutation in NEMO (K277A) and demonstrated that while wild type NEMO did not activate NFκB, NEMOK277A potently activated this transcription factor even though mutant and wild-type NEMO expressed to equivalent levels (Fig. 7E and 7F). Interestingly, MC005 inhibited the constitutively active of NEMOK277A suggesting that MC005 binding to active NEMO prevents NEMO conferring conformational priming to IKKβ. We next examined the direct consequences of MC005 binding to active NEMO by stimulating the metallothionein-inducible MC005 stable cells used previously (Fig. 5A) with TNFα and observed that while TNF-induced the IKK phosphorylation, IkB degradation and p65 phosphorylation necessary for NFκB activation, inducing the expression of MC005 inhibited all of these events (Fig. 7G).

The above data, taken in aggregate, suggest a model whereby MC005 binds NEMO and inhibits the activity of the conformational state that NEMO assumes on binding ubiquitin chains which normally primes IKKβ for the phosphorylation events required for full catalytic activity (Fig. 8). Thus MC005 binding to NEMO prevents IKKβ from phosphorylating IκBα and p65 thus inhibiting NFκB activation and the induction of NFκB-dependent gene expression. MC005 inhibition of active NEMO provides a rationale for inhibition of type I interferon, cytokine and chemokine production after primary virus sensing and pro-inflammatory cytokine stimulation.

Discussion

MCV is a common, dermatotropic poxvirus that causes benign skin neoplasms in humans with a more serious presentation in immunocompromised individuals like HIV patients (6). Compared to other poxviruses like VACV, which causes local inflammation in human skin lesions (28), MCV causes less of an inflammatory response. One factor contributing to this may be that fact that MCV forms histologically distinct, walled-off lesions that are less accessible to the immune system. However, keratinocytes present in such lesions do have efficient viral sensing machinery, suggesting that MCV is better equipped than poxviruses like VACV to suppress human innate immunity as a result of long-term co-evolution and adaptation to human infection. NFκB has a critical role in virus sensing pathways and initiating both virus-induced inflammation and the adaptive response to viruses, and notwithstanding the ability of VACV to trigger local inflammation in skin lesions, VACV possesses numerous immunomodulatory proteins including at least 10 inhibitors of NFκB, with evidence of others yet to be identified (29). In contrast, prior to this study, fewer than ten MCV immunomodulators had been reported, and only three of these affect NFκB activation, through partially characterized mechanisms (7, 30-32). We recently reported the discovery of an additional inhibitor, MC132, which inhibits NFκB by targeting the p65 subunit for proteasomal degradation by recruiting host Cullin-5/Elongin B/Elongin C complex (7). Although MCV research has been hampered by the lack of an animal or cell line infection model, analysis of the function of isolated ORFs expressed in cell lines has previously revealed important insights into how MCV proteins suppress host immunity (6, 7).

Since the study of poxvirus immunoregulators that inhibit the host response has been instructive in defining host-pathogen interactions and discovering new aspects of innate immunity (3), MCV, having co-evolved to specifically inhibit human immunity, is

481 unparalleled as a model poxvirus for understanding human innate immunity. Thus we
482 screened isolated MCV ORFs for effects on known anti-viral innate immune signaling
483 pathways in human cells and here report the discovery of MC005 from MCV subtype I as an
484 inhibitor of NFκB activation. MC005 is a small 89 amino acid protein (9kDa) encoded by
485 *MC005L* which is located on the left-hand terminus of the MCV genome, has no orthologues
486 in any other known poxviruses and exhibits no similarity to any other proteins.

487 TLR and cytosolic nucleic acid detection PRRs are critically involved in initial viral
488 sensing and type I IFN induction, while IL-1 and TNF production and subsequent signaling
489 regulates virus-induced inflammation which is required for mounting a full adaptive response
490 leading to virus clearance (3). Compellingly, MC005, like MC132, inhibited both PRR and
491 inflammatory cytokine signaling to NFκB activation, as well as suppressing NFκB activation
492 and chemokine production following poxviral or RNA virus infection.

493 Through systematic mapping of these pathways, we tracked the inhibitory effect of
494 MC005 to the IKK complex and determined that it specifically interacted with NEMO, the
495 regulatory subunit of the complex. As a focal point in IFN induction and inflammatory
496 signaling, the subunits of the IKK complex are commonly targeted by viruses (33). The MCV
497 protein MC159 has previously been shown to interact specifically with NEMO to inhibit
498 NFκB activation (30), however the authors did not describe in detail how MC159 interacts
499 with NEMO and inhibits IKK activation. Interestingly, although the cGAS-STING pathway
500 induces NFκB-dependent genes, the mechanisms whereby STING activates NFκB is
501 unknown. Since MC005 inhibited cGAS-stimulated NFκB activation, this suggest that
502 NEMO does have a role in this pathway.

503 As our current understanding of the precise dynamic mechanism by which the IKK
504 complex is activated is incomplete we are in need of new tools to bolster existing models of
505 activation of this critical regulatory crux in innate immunity and inflammation. What is clear

is that ubiquitin chains (linked to upstream signaling proteins) serve as a 'code' which is 'read' and translated into a signal by ubiquitin binding proteins like NEMO (which binds K63-linked and Met1-linked polyubiquitin chains) as well as TAB2/3 (which binds K63-linked polyubiquitin chains only) and several lines of evidence demonstrate that ubiquitin binding by these proteins is essential for activation of the IKK complex (22, 34, 35). This requirement for ubiquitin binding appears to be not solely for generating a scaffold for co-clustering IKK and TAB/TAK complexes, rather it also appears to be required for priming these complexes for cross- and auto-phosphorylation by via conformational changes within complexes. A comparison of the crystal structure of the free and ubiquitin-bound form of the NEMO UBAN domain revealed that ubiquitin-binding induced a straightening of the CC2 domain (36) and these authors suggest that this may function as an allosteric means of inducing or conducting a conformational change in the IKK subunits of the mutimeric complex to a form capable of autophosphorylation and phosphorylation by TAK1. Indeed, a single point mutation in the CC2 domain of murine NEMO (K270A) makes the IKK complex constitutively active without the requirement for ubiquitin binding by forcing NEMO into a conformation that simulates the ubiquitin bound state (27). We observed that MC005 inhibited the constitutively active equivalent human point mutant of NEMO (K277A).

We also demonstrated that MC005 binds to a point in NEMO directly between the regions that mediate IKK binding and ubiquitin binding. This binding does not impair NEMO dimerisation in the multimeric IKK complex, nor does it prevent the binding of NEMO to ubiquitin. As the IKKs bind within the first half of the CC1 domain and the current model of IKK activation suggests that UBAN-ubiquitin binding causes a conformational straightening of the CC2 domain which induces a conformational repositioning of the IKKs priming them for phosphorylation by TAK1, we propose that MC005, by binding between these two regions inhibits the conduction of this conformational signal within NEMO. Thus the viral

protein not only serves as a way of better understanding how MCV inhibits virus sensing and inflammation in human tissue but also serves as a useful tool for validating the evolutionarily conserved structural mechanism by which the IKK is regulated and activated. This better understanding might inform therapeutic strategies for inhibiting the IKK complex in inflammatory and autoimmune disease.

Interestingly, the sequence of MC005 differs between MCV subtype I and II. While subtypes I and IV are the most common in infection of immunocompetent individuals, subtype II is more common in HIV patients (37, 38) in whom MCV causes a more severe, disseminated disease and is a good indicator of advancing immunosuppression (39). The subtype II MC005 variant is shorter than type I, including a 7 amino acid C-terminal deletion and several conservative and non-conservative amino acid differences (residues 41, 44, 54 and 55) which lie within the region we have determined is required for inhibitory activity (residues 11-57). It is possible that disrupted or altered activity of MC005 in MCV subtype II may affect the dynamics of infection in immunocompromised hosts explaining this difference in its tropism and presentation.

Overall our analysis of the MCV genome for ORFs that affect human signaling networks culminating in activation of NFκB, revealed MC005, an inhibitor of PRR- and cytokine-activated NFκB, unique to MCV amongst poxviruses, and delineated the precise mechanism of its action within the known dynamics of IKK complex regulation. Thus, now four MCV proteins have now been shown to target NFκB activation, namely MC159, MC160, MC132 and MC005. Further screening of the MCV genome for novel inhibitors of human innate immunity will likely reveal additional inhibitors of innate immune signaling, novel details of the signaling pathways they antagonize and may present new strategies for selective inhibition of sensing and inflammatory events in disease.

Acknowledgements

This work was supported by Science Foundation Ireland grant 11/PI/1056 (to A.G.B.), the Max-Planck Free Floater program (to A.P.), the ERC (StG 311339 – iViP, to A.P.) and Marie Curie Intra-European Fellowship no. 332057 (to G.B. and A.G.B). PJF is partly supported by funding from the Imperial NIHR Biomedical Research Centre.

References

1. **Gurtler C, Bowie AG.** 2013. Innate immune detection of microbial nucleic acids. Trends Microbiol **21:**413-420.
2. **Bowie AG, Unterholzner L.** 2008. Viral evasion and subversion of pattern-recognition receptor signalling. Nat Rev Immunol **8:**911-922.
3. **Brady G, Bowie AG.** 2014. Innate immune activation of NFkappaB and its antagonism by poxviruses. Cytokine Growth Factor Rev **25:**611-620.
4. **Senkevich TG, Koonin EV, Bugert JJ, Darai G, Moss B.** 1997. The genome of molluscum contagiosum virus: analysis and comparison with other poxviruses. Virology **233:**19-42.
5. **Struzik J, Szulc-Dabrowska L, Niemialtowski M.** 2014. Modulation of NFkB transcription factor activation by Molluscum contagiosum virus proteins. Postepy Hig Med Dosw (Online) **68:**129-136.
6. **Chen X, Anstey AV, Bugert JJ.** 2013. Molluscum contagiosum virus infection. Lancet Infect Dis **13:**877-888.
7. **Brady G, Haas DA, Farrell PJ, Pichlmair A, Bowie AG.** 2015. Poxvirus Protein MC132 from Molluscum Contagiosum Virus Inhibits NF-B Activation by Targeting p65 for Degradation. J Virol **89:**8406-8415.
8. **Bugert JJ, Lohmuller C, Darai G.** 1999. Characterization of early gene transcripts of molluscum contagiosum virus. Virology **257:**119-129.
9. **Chinnakannan SK, Nanda SK, Baron MD.** 2013. Morbillivirus v proteins exhibit multiple mechanisms to block type 1 and type 2 interferon signalling pathways. PLoS One **8:**e57063.
10. **Hubner NC, Bird AW, Cox J, Splettstoesser B, Bandilla P, Poser I, Hyman A, Mann M.** 2010. Quantitative proteomics combined with BAC TransgeneOmics reveals in vivo protein interactions. J Cell Biol **189:**739-754.
11. **Pascutti MF, Rodriguez AM, Falivene J, Giavedoni L, Drexler I, Gherardi MM.** 2011. Interplay between modified vaccinia virus Ankara and dendritic cells: phenotypic and functional maturation of bystander dendritic cells. J Virol **85:**5532-5545.
12. **Yeruva S, Ramadori G, Raddatz D.** 2008. NF-kappaB-dependent synergistic regulation of CXCL10 gene expression by IL-1beta and IFN-gamma in human intestinal epithelial cell lines. Int J Colorectal Dis **23:**305-317.
13. **Ablasser A, Goldeck M, Cavlar T, Deimling T, Witte G, Rohl I, Hopfner KP, Ludwig J, Hornung V.** 2013. cGAS produces a 2'-5'-linked cyclic dinucleotide second messenger that activates STING. Nature **498:**380-384.
14. **Sun L, Wu J, Du F, Chen X, Chen ZJ.** 2013. Cyclic GMP-AMP synthase is a cytosolic DNA sensor that activates the type I interferon pathway. Science **339:**786-791.
15. **Dai P, Wang W, Cao H, Avogadri F, Dai L, Drexler I, Joyce JA, Li XD, Chen Z, Merghoub T, Shuman S, Deng L.** 2014. Modified Vaccinia Virus Ankara Triggers Type I IFN Production in

Murine Conventional Dendritic Cells via a cGAS/STING-Mediated Cytosolic DNA-Sensing Pathway. PLoS Pathog **10:**e1003989.

16. **Ablasser A, Schmid-Burgk JL, Hemmerling I, Horvath GL, Schmidt T, Latz E, Hornung V.** 2013. Cell intrinsic immunity spreads to bystander cells via the intercellular transfer of cGAMP. Nature **503:**530-534.
17. **Valentine R, Smith GL.** 2010. Inhibition of the RNA polymerase III-mediated dsDNA-sensing pathway of innate immunity by vaccinia virus protein E3. J Gen Virol **91:**2221-2229.
18. **Hutchens M, Luker KE, Sottile P, Sonstein J, Lukacs NW, Nunez G, Curtis JL, Luker GD.** 2008. TLR3 increases disease morbidity and mortality from vaccinia infection. J Immunol **180:**483-491.
19. **Samuelsson C, Hausmann J, Lauterbach H, Schmidt M, Akira S, Wagner H, Chaplin P, Suter M, O'Keeffe M, Hochrein H.** 2008. Survival of lethal poxvirus infection in mice depends on TLR9, and therapeutic vaccination provides protection. J Clin Invest **118:**1776-1784.
20. **Ku JK, Kwon HJ, Kim MY, Kang H, Song PI, Armstrong CA, Ansel JC, Kim HO, Park YM.** 2008. Expression of Toll-like receptors in verruca and molluscum contagiosum. J Korean Med Sci **23:**307-314.
21. **McDermott EP, O'Neill LA.** 2002. Ras participates in the activation of p38 MAPK by interleukin-1 by associating with IRAK, IRAK2, TRAF6, and TAK-1. J Biol Chem **277:**7808-7815.
22. **Clark K, Nanda S, Cohen P.** 2013. Molecular control of the NEMO family of ubiquitin-binding proteins. Nat Rev Mol Cell Biol **14:**673-685.
23. **Skaug B, Jiang X, Chen ZJ.** 2009. The role of ubiquitin in NF-kappaB regulatory pathways. Annu Rev Biochem **78:**769-796.
24. **Ivins FJ, Montgomery MG, Smith SJ, Morris-Davies AC, Taylor IA, Rittinger K.** 2009. NEMO oligomerization and its ubiquitin-binding properties. Biochem J **421:**243-251.
25. **Tegethoff S, Behlke J, Scheidereit C.** 2003. Tetrameric oligomerization of IkappaB kinase gamma (IKKgamma) is obligatory for IKK complex activity and NF-kappaB activation. Mol Cell Biol **23:**2029-2041.
26. **Polley S, Huang DB, Hauenstein AV, Fusco AJ, Zhong X, Vu D, Schrofelbauer B, Kim Y, Hoffmann A, Verma IM, Ghosh G, Huxford T.** 2013. A structural basis for IkappaB kinase 2 activation via oligomerization-dependent trans auto-phosphorylation. PLoS Biol **11:**e1001581.
27. **Bloor S, Ryzhakov G, Wagner S, Butler PJ, Smith DL, Krumbach R, Dikic I, Randow F.** 2008. Signal processing by its coil zipper domain activates IKK gamma. Proc Natl Acad Sci U S A **105:**1279-1284.
28. **Wlodaver CG, Palumbo GJ, Waner JL.** 2004. Laboratory-acquired vaccinia infection. J Clin Virol **29:**167-170.
29. **Sumner RP, Maluquer de Motes C, Veyer DL, Smith GL.** 2014. Vaccinia virus inhibits NF-kappaB-dependent gene expression downstream of p65 translocation. J Virol **88:**3092-3102.
30. **Randall CM, Jokela JA, Shisler JL.** 2012. The MC159 protein from the molluscum contagiosum poxvirus inhibits NF-kappaB activation by interacting with the IkappaB kinase complex. J Immunol **188:**2371-2379.
31. **Nichols DB, Shisler JL.** 2006. The MC160 protein expressed by the dermatotropic poxvirus molluscum contagiosum virus prevents tumor necrosis factor alpha-induced NF-kappaB activation via inhibition of I kappa kinase complex formation. J Virol **80:**578-586.
32. **Murao LE, Shisler JL.** 2005. The MCV MC159 protein inhibits late, but not early, events of TNF-alpha-induced NF-kappaB activation. Virology **340:**255-264.
33. **Amaya M, Keck F, Bailey C, Narayanan A.** 2014. The role of the IKK complex in viral infections. Pathog Dis **72:**32-44.
34. **Husnjak K, Dikic I.** 2012. Ubiquitin-binding proteins: decoders of ubiquitin-mediated cellular functions. Annu Rev Biochem **81:**291-322.

35. **Kulathu Y, Komander D.** 2012. Atypical ubiquitylation - the unexplored world of polyubiquitin beyond Lys48 and Lys63 linkages. Nat Rev Mol Cell Biol **13:**508-523.
36. **Rahighi S, Ikeda F, Kawasaki M, Akutsu M, Suzuki N, Kato R, Kensche T, Uejima T, Bloor S, Komander D, Randow F, Wakatsuki S, Dikic I.** 2009. Specific recognition of linear ubiquitin chains by NEMO is important for NF-kappaB activation. Cell **136:**1098-1109.
37. **Thompson CH, de Zwart-Steffe RT, Donovan B.** 1992. Clinical and molecular aspects of molluscum contagiosum infection in HIV-1 positive patients. Int J STD AIDS **3:**101-106.
38. **Yamashita H, Uemura T, Kawashima M.** 1996. Molecular epidemiologic analysis of Japanese patients with molluscum contagiosum. Int J Dermatol **35:**99-105.
39. **Gur I.** 2008. The epidemiology of Molluscum contagiosum in HIV-seropositive patients: a unique entity or insignificant finding? Int J STD AIDS **19:**503-506.

662 **Figure Legends**

663

664 **Figure 1. Inhibition of cytosolic nucleic acid sensing pathway and virus-stimulated**
665 **NFκB activation by MC005.**

666 (A) THP-1 cells were transduced with lentiviruses containing empty vector or MC005-
667 FLAG -expressing constructs and stable cells were generated. Extracts from cells were
668 probed for expression of MC005- FLAG. Stable THP-1 cells were seeded at 1 x 10^6 cells per
669 ml and transfected with (B) 1μg/ml poly (dA:dT) or (C) infected with SeV for 24 hours.
670 Supernatants were harvested from cells and IP-10 production was assayed by ELISA. (D)
671 Localization of MC005 HEK293T cells. Cells were transfected with 3 μg pCEP4-MC005-
672 FLAG vector. Cells were fixed 24 hours later, and stained with DAPI (blue) or for MCV
673 protein expression (green). Representative images shown (n=4). (E-L) HEK293T cells were
674 seeded at 2 x 10^5 cells per ml and transfected with indicated reporter genes and 25 or 50ng of
675 empty vector (control) or pCEP4 plasmids expressing MC005-FLAG or MC014-FLAG
676 (indicated by a wedge). Cells were then infected with (E, M) MVA (G) SeV or (L) VSV for
677 16 hours or transfected with (H, I) 25ng cGAS and 25ng STING or (J) 1μg/ml poly (dA:dT).
678 NFκB or ISRE reporter activity was assayed 24 hours later. Data are mean ± SD of triplicate
679 samples from a representative experiment (n = 3). * $p<0.001$ compared to control.

680

681 **Figure 2. Inhibition of TLR-dependent NFκB activation by MC005.**

682 Effect of MC005 on TLR9/3-stimulated NFκB activation. HEK293T cells were seeded at 2 x
683 10^5 cells per ml and transfected with 80 ng NFκB or ISRE reporter gene, 40 ng TK renilla
684 reporter gene and 25 or 50 ng (indicated by wedge) empty vector (control) or pCEP4
685 plasmids expressing the indicated MCV ORFs and CD4-TLR9 (A, B), CD4-TLR3 (C, D) or
686 TRIF (E, F). Cells were harvested 24 hours later and assayed for reporter gene activity. Data

687 is % activity of stimulation for control cells, and is mean ± SD of triplicate samples from a
688 representative experiment (n = 3). * $p<0.001$ compared to control.
689
690 **Figure 3. MC005 inhibition of pro-inflammatory cytokine-stimulated NFκB activation**
691 **downstream of TRAFs.**
692 Effect of MC005 on TNF-stimulated NFκB activation. (A) HEK293T cells were seeded at 2
693 x 10^5 cells per ml and transfected with 80 ng NFκB reporter gene, 40 ng TK renilla reporter
694 gene and 25 or 50 ng (indicated by wedge) empty vector (control) or pCEP4 plasmids
695 expressing the indicated MCV ORFs were stimulated with 50 ng/ml TNFα for 6 h then
696 harvested and assayed for NFκB reporter gene activity. Data is % activity of stimulation for
697 control cells, and is mean ± SD of triplicate samples from a representative experiment (n =
698 4). (B) Extracts from experiment (A) samples were probed for expression of FLAG-tagged
699 viral proteins. (C) Elk1 activation by Ras was measured by reporter gene assay, in cells
700 transfected with empty vector (control) or pCEP4 plasmids expressing MCV ORFs. (D-F) As
701 for (A) except HEK293T (D), COS-1 (E) or HeLa (F) cells were transfected with 50ng
702 TRAF2-FLAG instead of TNFα stimulation. (G, H) Stable cells containing pCEP4 empty
703 vector or pCEP4-MC005-FLAG and expression of FLAG-tagged protein was probed (G).
704 Stable cells were then seeded at 2 x 10^5 cells per ml and stimulated with 50 ng/ml TNFα for
705 24 h. IL-8 production was then assayed by ELISA (H). (I) Effect of MC005 on IL1-
706 stimulated NFκB activation. As for (A) except cells were stimulated with 50ng/ml IL1β. (J)
707 Extracts from experiment (I) samples were probed for expression of FLAG tagged viral
708 proteins. (K) as for (A) except cells were transfected with 50 ng plasmid expressing TRAF6.
709 Data is % activity of stimulation for control cells, and is mean ± SD of triplicate samples
710 from a representative experiment (n = 3). * $p<0.001$ compared to control.
711

712 **Figure 4. MC005 inhibits PRR- and cytokine-stimulated NFκB activation at a point**
713 **proximal to the IKK complex.**
714 (A) Schematic showing multiple signal transduction pathways to NFκB expected to be
715 activated during a poxviral infection, all of which are shown to be sensitive to MC005
716 inhibition (Figures 1-3) and by MC132 targeting of p65. After generation of ubiquitin chains,
717 three key regulatory events occur leading to canonical NFκB activation. (1) The IKK
718 complex (through NEMO) and the TAB/TAK complex (through the TABs) bind to ubiquitin
719 chains. (2) ubiquitin-binding of NEMO induces a conformational change which affects the
720 entire IKK complex presenting the IKKs for autophosphorylation and phosphorylation by
721 TAK1. (3) Active phosphor-IKKβ dual phosphorylates both p65 and IκBα (triggering its
722 degradation) leading to nuclear translocation of NFκB and induction of anti-viral and pro-
723 inflammatory gene expression. (B-D) Comparison of MC005 with MC132 inhibition of
724 signaling events surrounding IKK complex activation. HEK293T cells were seeded at 2 x 10^5
725 cells per ml and transfected with 50 ng empty vector (control) or pCEP4 plasmids expressing
726 the indicated MCV ORFs together with (B) 10ng TAB2 (C) 10ng IKKβ or (D) 5ng p65 were
727 then harvested and assayed for NFκB reporter gene activity 24 hours later. Data is % activity
728 of stimulation for control cells, and is mean ± SD of triplicate samples from a representative
729 experiment (n = 3). * $p<0.001$ compared to control.
730
731 **Figure 5. MC005 interacts with NEMO**
732 Analysis of cellular MC005-interacting proteins. (A) HEK293T cells stably transfected with
733 pMEP4-MC005 and treated with (+) or without (-) 1 μM $CdCl_2$ to induce expression. Lysates
734 were probed for FLAG protein expression. (B) Volcano plot of MC005-interacting proteins
735 identified by AP-MS from MC005-expressing HEK293T cells. (C-E) MC005 interacts with
736 NEMO and the IKK complex. HEK293T (C) or Hela (D) cells were seeded at 4 x 10^6 cells

per 10cm plate and transfected with 4 μg expression vectors for NEMO-HA and MC005-FLAG as indicated. 24 h later cells were lysed and immunoprecipitated with anti-FLAG beads then immunoblotted with the indicated antibodies. Representative blots are shown (n = 3). (E) Hela cells seeded in 24 well dishes on coverslips were transfected with 0.5 μg of expression vectors for NEMO- FLAG, IKKβ- FLAG and MC005- FLAG. Cells were fixed 24 hours later, and stained with DAPI (blue) or for HA (red) and FLAG (green). MC005 interacts with TRAF6 through NEMO association. (F) As for (C) except cells were transfected with NEMO-HA, MC005-HA and TRAF6- FLAG. Representative blots are shown (n = 3).

Figure 6. Inhibition of NFκB by MC005 requires a central 46 amino acid region

(A) Generation of MC005 truncations. Constructs expressing MC005 truncations were generated by truncation at the indicated position in the protein. Region and sequence required for activity indicated at top and region marked in truncations by vertical lines. (B) Interaction of MC005 and truncations with NEMO correlates with inhibitory activity. Cells were seeded at 4 x 10^6 cells per 10cm plate and transfected with 4 μg expression vectors for NEMO-HA and MC005- FLAG as indicated. 24 h later cells were lysed and immunoprecipitated with anti-FLAG beads then immunoblotted with the indicated antibodies. Representative blot is shown (n = 3). (C) Central 46 amino acid region of MC005 required for NFκB inhibition. HEK293T cells were seeded at 2 x 10^5 cells per ml and transfected with 80 ng NFκB, 40 ng TK renilla reporter gene, 10ng TRAF6 and 50 ng empty vector (control) or pCEP4 plasmids expressing MC005 and truncations. Cells were harvested 24 hours later and assayed for reporter gene activity. Data is % activity of stimulation for control cells, and is mean ± SD of triplicate samples from a representative experiment (n = 3). * $p<0.001$ compared to control.

Figure 7. MC005 prevents ubiquitin-activated NEMO from positively regulating IKKβ. MC005 binds the second half of the NEMO CC1 domain (A) Generation of NEMO truncations. Regions of note in NEMO: 'Dimer' region (1-80), 'IKK binding' (40-120) and 'UBAN' domain (249-339). Coiled coil (CC), leucine zipper (LZ) and zinc finger (ZF) regions also indicated. Constructs expressing NEMO truncations were generated by truncation at the indicated positions in the protein. (B) Cells were seeded at 4 x 10^6 cells per 10cm plate and transfected with 4 μg expression vectors for NEMO-HA, NEMO truncation-HA and MC005- FLAG as indicated. 24 h later cells were lysed and immunoprecipitated with anti-FLAG beads then immunoblotted with the indicated antibodies. Representative blot is shown (n = 3). MC005 does not disrupt NEMO unibquitination or association with ubiquitinated proteins. (C) Cells were seeded at 4 x 10^6 cells per 10cm plate and transfected with 4 μg expression vectors for NEMO- FLAG, ubiquitin-HA and MC005-HA as indicated. 24 h later cells were lysed and immunoprecipitated with anti-FLAG beads then immunoblotted with the indicated antibodies. Representative blot is shown (n = 3). Arrow indicates ubiquitinated NEMO. MC005 does not prevent IKK complex assembly. (D) Cells were seeded at 4 x 10^6 cells per 10cm plate and transfected with 4 μg expression vectors for NEMO-HA, NEMO- FLAG and MC005-HA as indicated. 24 h later, cells were lysed and immunoprecipitated with anti-FLAG beads then immunoblotted with the indicated antibodies. Representative blot is shown (n = 3). (E, F) Constitutively active NEMOK277A mutant simulating conformation of ubiquitin-bound NEMO is inhibited by MC005. (E) HEK293T cells were seeded at 2 x 10^5 cells per ml and transfected with 80 ng NFκB, 40 ng TK renilla reporter gene, 50ng NEMO or NEMOK277A and 25 or 50 ng (indicated by wedge) empty vector (control) or pCEP4 plasmids expressing MC005. Cells were harvested 24 hours later and assayed for reporter gene activity. Data is % activity of stimulation for control cells, and is mean ± SD of triplicate samples from a representative experiment (n =

787 3). (F) Extracts from experiment (E) samples were probed for expression of FLAG -tagged
788 MC005. MC005 interaction with IKK complex inhibits IKKβ and p65 phosphorylation and
789 IκB degradation. (G) (HEK293T cells stably transfected with pMEP4 and pMEP4-MC005,
790 were seeded at 6 x 10^5 cells per well in 6-well dishes and treated with (+) or without (-) 1 μM
791 $CdCl_2$ to induce MCV protein expression. 24 h later cells were stimulated with 50 ng/ml
792 TNFα for the indicated times, and cell lysates immunoblotted with the indicated antibodies.
793 Representative blots shown (n=3). * $p<0.001$ compared to control.
794
795 **Fig. 8. Model for MC005-mediated inhibition of human NFκB signaling.**
796 PRR virus sensing and cytokine signaling pathways drive polyubiquitination events required
797 for IKK complex activation. NEMO subunits bind TRAF-generated ubiquitin chains which
798 induces a conformational change within NEMO, and a subsequent conformational change
799 and rearrangement within the IKK complex leading to presentation of the IKKs (e.g. IKKβ)
800 for phosphorylation by TAK1 and auto-phosphorylation. MC005 inhibits IKK complex
801 activation by binding to active NEMO and preventing the conformational signal (induced by
802 ubiquitin binding) from priming the IKKs for subsequent activation.
803

Figure 1

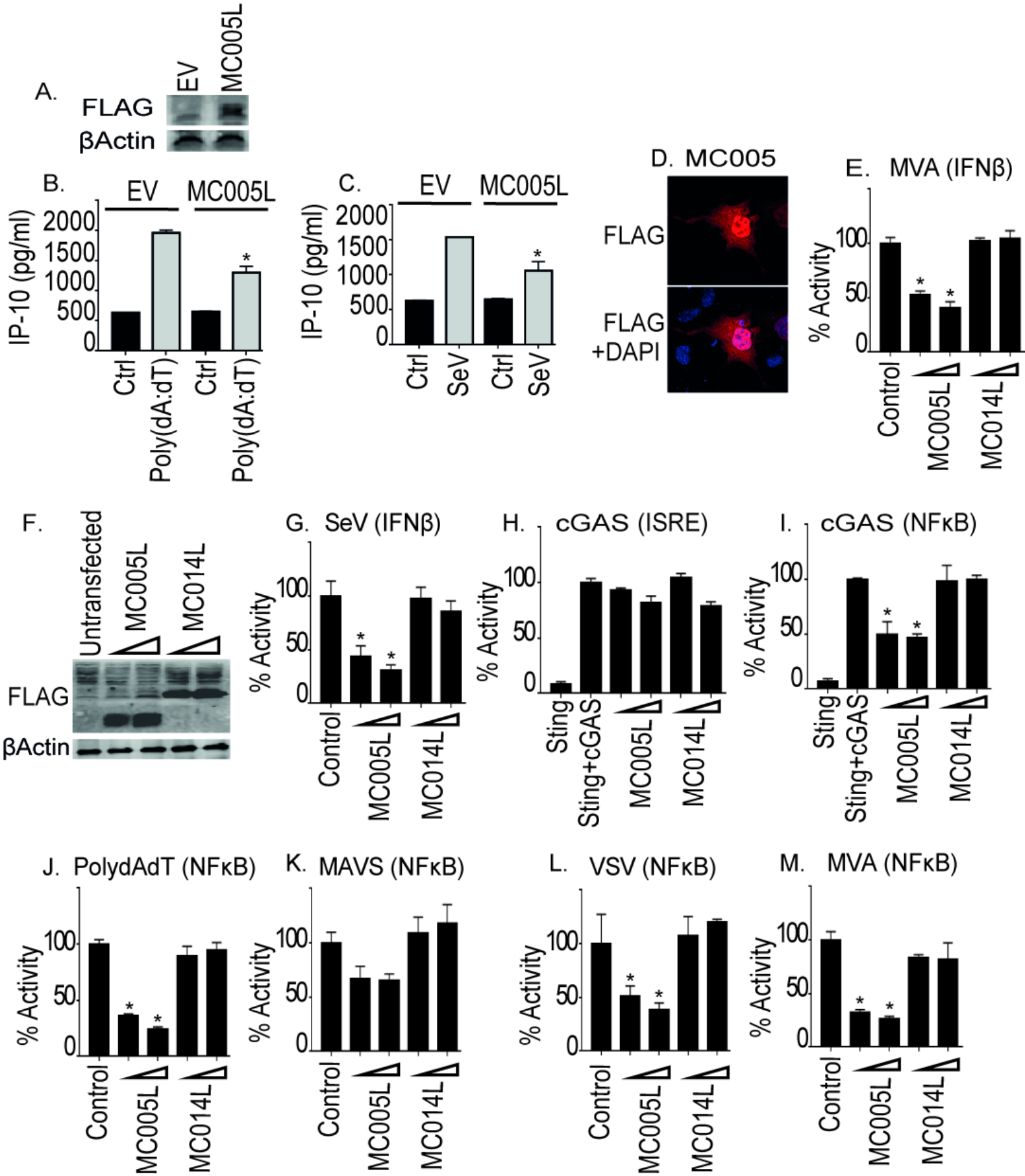
A.
EV
MC005L
FLAG
βActin
B.
EV
MC005L
IP-10 (pg/ml)
2000
1500
1000
500
0
Ctrl
Poly(dA:dT)
Ctrl
Poly(dA:dT)
C.
EV
MC005L
IP-10 (pg/ml)
2000
1500
1000
500
0
Ctrl
SeV
Ctrl
SeV
D. MC005
FLAG
FLAG
+DAPI
E. MVA (IFNβ)
% Activity
100
50
0
Control
MC005L
MC014L
F.
Untransfected
MC005L
MC014L
FLAG
βActin
G. SeV (IFNβ)
% Activity
100
50
0
Control
MC005L
MC014L
H. cGAS (ISRE)
% Activity
100
50
0
Sting
Sting+cGAS
MC005L
MC014L
I. cGAS (NFκB)
% Activity
100
50
0
Sting
Sting+cGAS
MC005L
MC014L
J. PolydAdT (NFκB)
% Activity
100
50
0
Control
MC005L
MC014L
K. MAVS (NFκB)
% Activity
100
50
0
Control
MC005L
MC014L
L. VSV (NFκB)
% Activity
100
50
0
Control
MC005L
MC014L
M. MVA (NFκB)
% Activity
100
50
0
Control
MC005L
MC014L

Figure 2

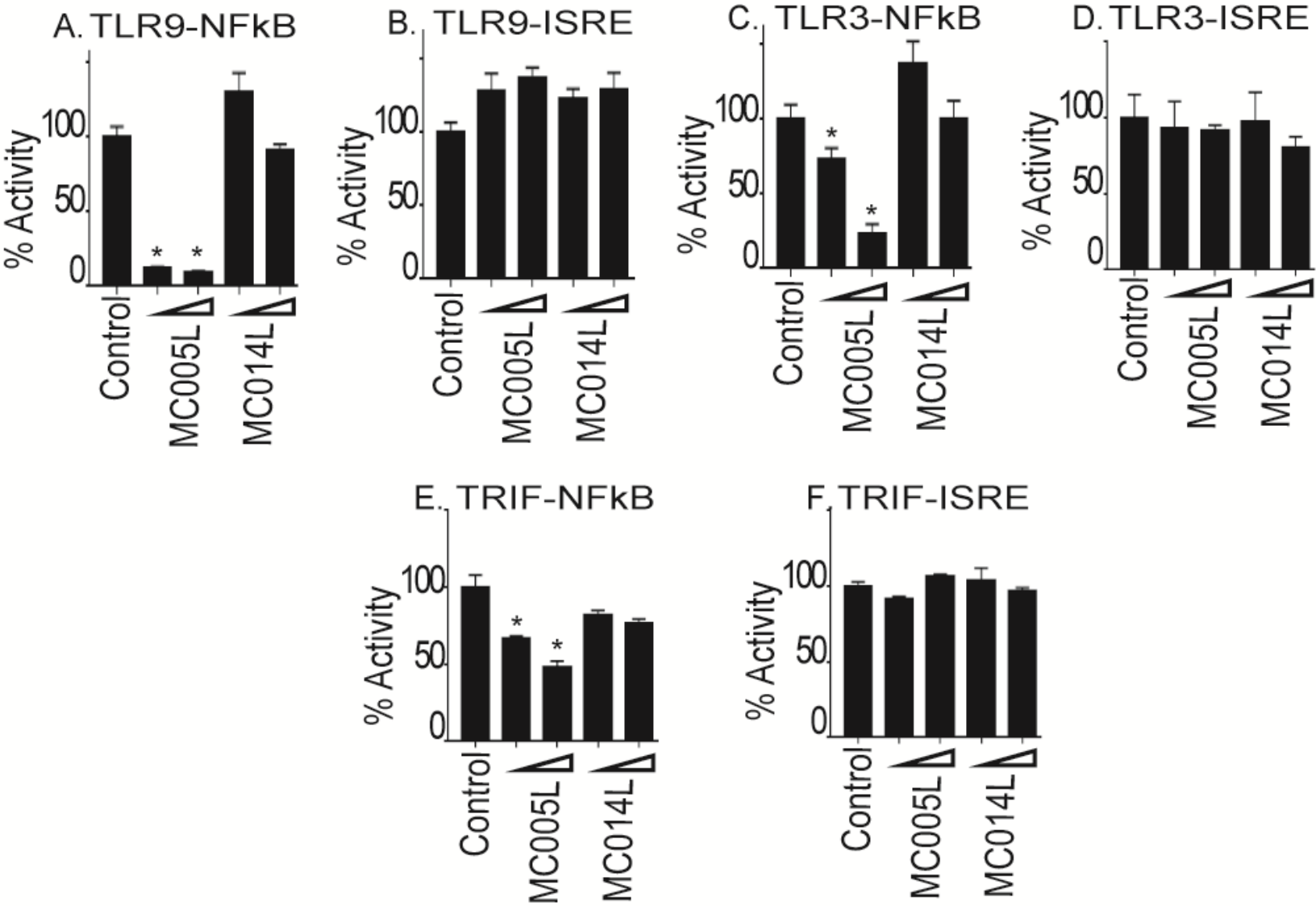
A. TLR9-NFkB
B. TLR9-ISRE
C. TLR3-NFkB
D. TLR3-ISRE
E. TRIF-NFkB
F. TRIF-ISRE
% Activity
100
50
0
*
Control
MC005L
MC014L

Figure 3

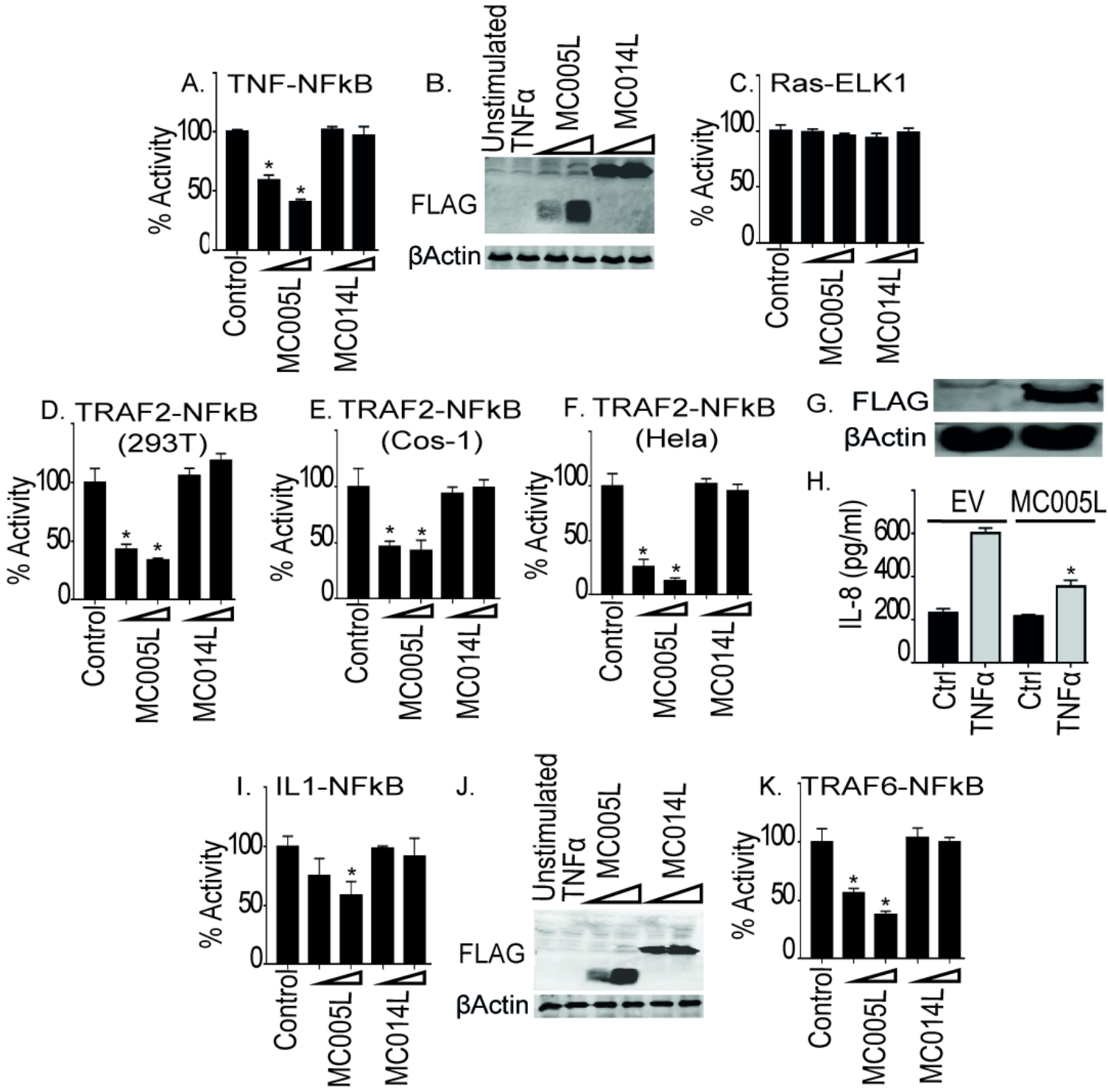
A. TNF-NFkB
% Activity
100
50
0
Control
MC005L
MC014L
B.
Unstimulated
TNFα
MC005L
MC014L
FLAG
βActin
C. Ras-ELK1
% Activity
100
50
0
Control
MC005L
MC014L
D. TRAF2-NFkB (293T)
% Activity
100
50
0
Control
MC005L
MC014L
E. TRAF2-NFkB (Cos-1)
% Activity
100
50
0
Control
MC005L
MC014L
F. TRAF2-NFkB (Hela)
% Activity
100
50
0
Control
MC005L
MC014L
G. FLAG
βActin
H.
EV
MC005L
IL-8 (pg/ml)
600
400
200
0
Ctrl
TNFα
Ctrl
TNFα
I. IL1-NFkB
% Activity
100
50
0
Control
MC005L
MC014L
J.
Unstimulated
TNFα
MC005L
MC014L
FLAG
βActin
K. TRAF6-NFkB
% Activity
100
50
0
Control
MC005L
MC014L

*

Figure 4

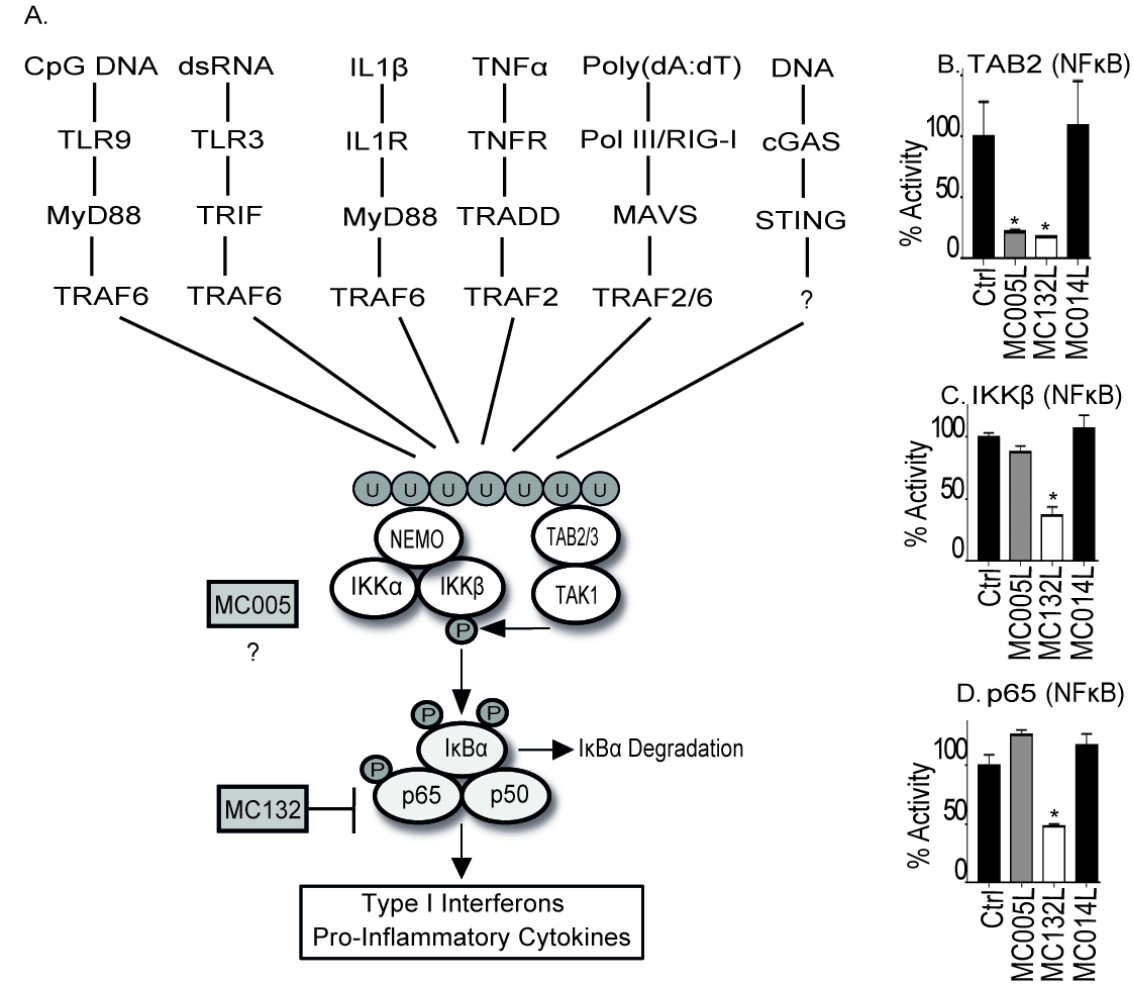
A.
CpG DNA
dsRNA
IL1β
TNFα
Poly(dA:dT)
DNA
TLR9
TLR3
IL1R
TNFR
Pol III/RIG-I
cGAS
MyD88
TRIF
MyD88
TRADD
MAVS
STING
TRAF6
TRAF6
TRAF6
TRAF2
TRAF2/6
?
U
NEMO
TAB2/3
IKKα
IKKβ
TAK1
P
MC005
?
IκBα
IκBα Degradation
p65
p50
MC132
Type I Interferons
Pro-Inflammatory Cytokines

B. TAB2 (NFκB)
% Activity
100
50
0
*
*
Ctrl
MC005L
MC132L
MC014L

C. IKKβ (NFκB)
% Activity
100
50
0
*
Ctrl
MC005L
MC132L
MC014L

D. p65 (NFκB)
% Activity
100
50
0
*
Ctrl
MC005L
MC132L
MC014L

Figure 5

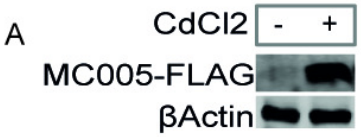
A
CdCl2
-
+
MC005-FLAG
βActin

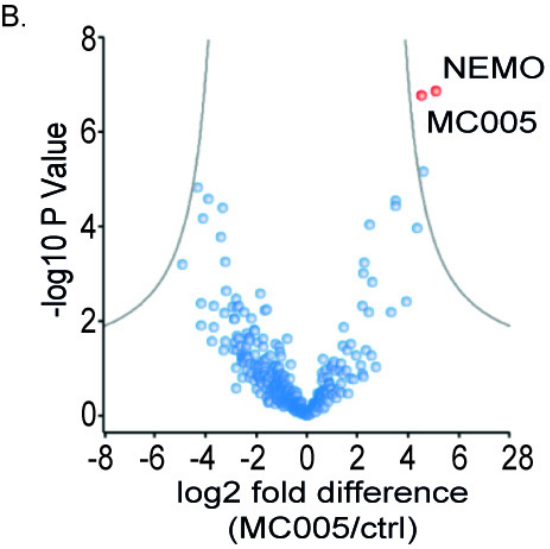
B.
8
6
4
2
0
-log10 P Value
NEMO
MC005
-8
-6
-4
-2
0
2
4
6
28
log2 fold difference
(MC005/ctrl)

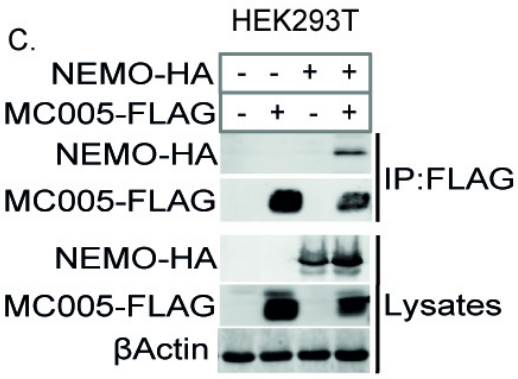
C.
HEK293T
NEMO-HA
MC005-FLAG
IP:FLAG
Lysates
βActin

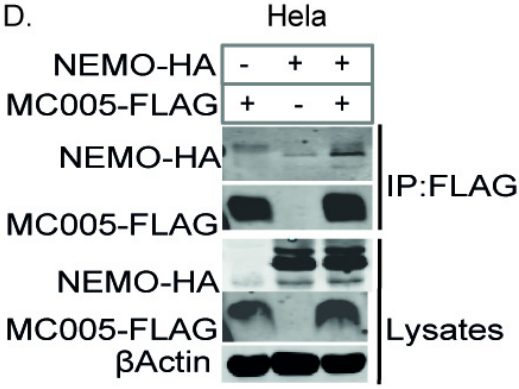
D.
Hela
NEMO-HA
MC005-FLAG
IP:FLAG
Lysates
βActin

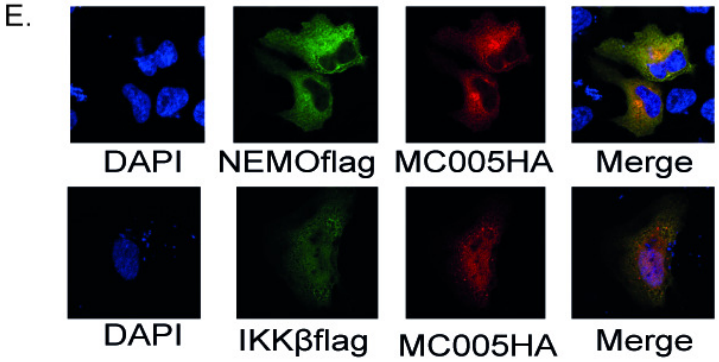
E.
DAPI
NEMOflag
MC005HA
Merge
DAPI
IKKβflag
MC005HA
Merge

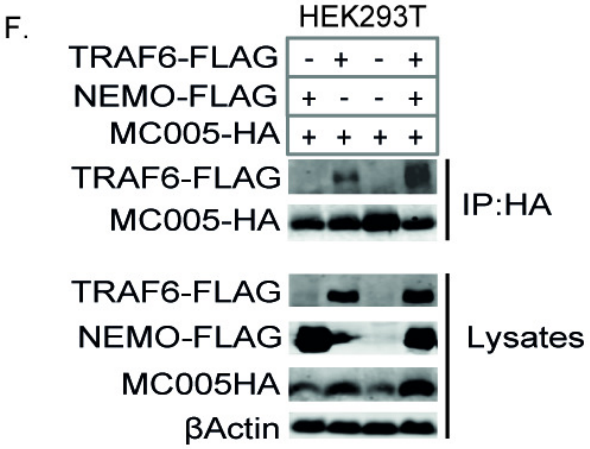
F.
HEK293T
TRAF6-FLAG
NEMO-FLAG
MC005-HA
IP:HA
Lysates
MC005HA
βActin

Figure 6.

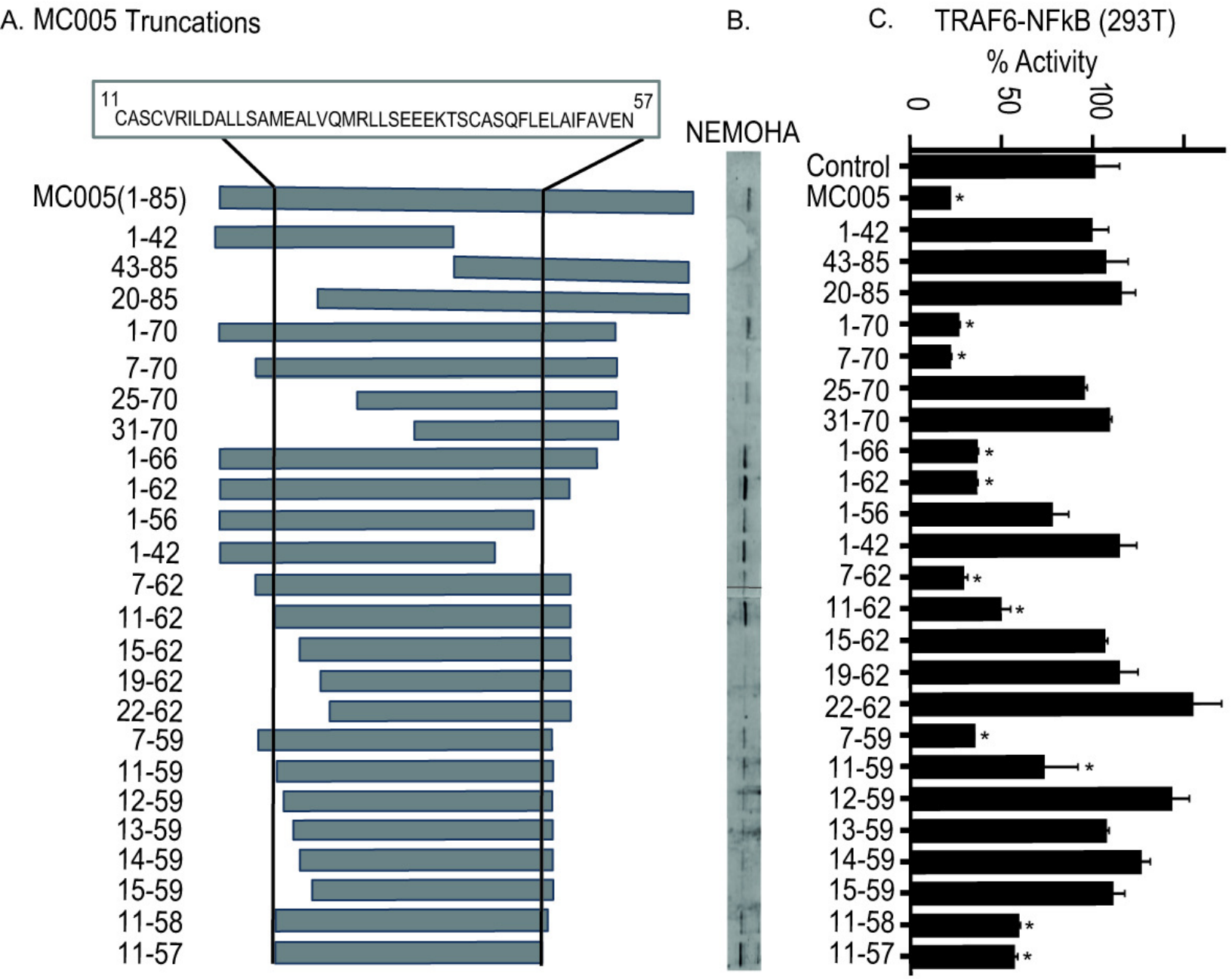
A. MC005 Truncations
11
CASCVRILDALLSAMEALVQMRLLSEEEKTSCASQFLELAIFAVEN
57
MC005(1-85)
1-42
43-85
20-85
1-70
7-70
25-70
31-70
1-66
1-62
1-56
1-42
7-62
11-62
15-62
19-62
22-62
7-59
11-59
12-59
13-59
14-59
15-59
11-58
11-57
B.
NEMOHA
C.
TRAF6-NFkB (293T)
% Activity
0
50
100
Control
MC005
1-42
43-85
20-85
1-70
7-70
25-70
31-70
1-66
1-62
1-56
1-42
7-62
11-62
15-62
19-62
22-62
7-59
11-59
12-59
13-59
14-59
15-59
11-58
11-57

Figure 7.

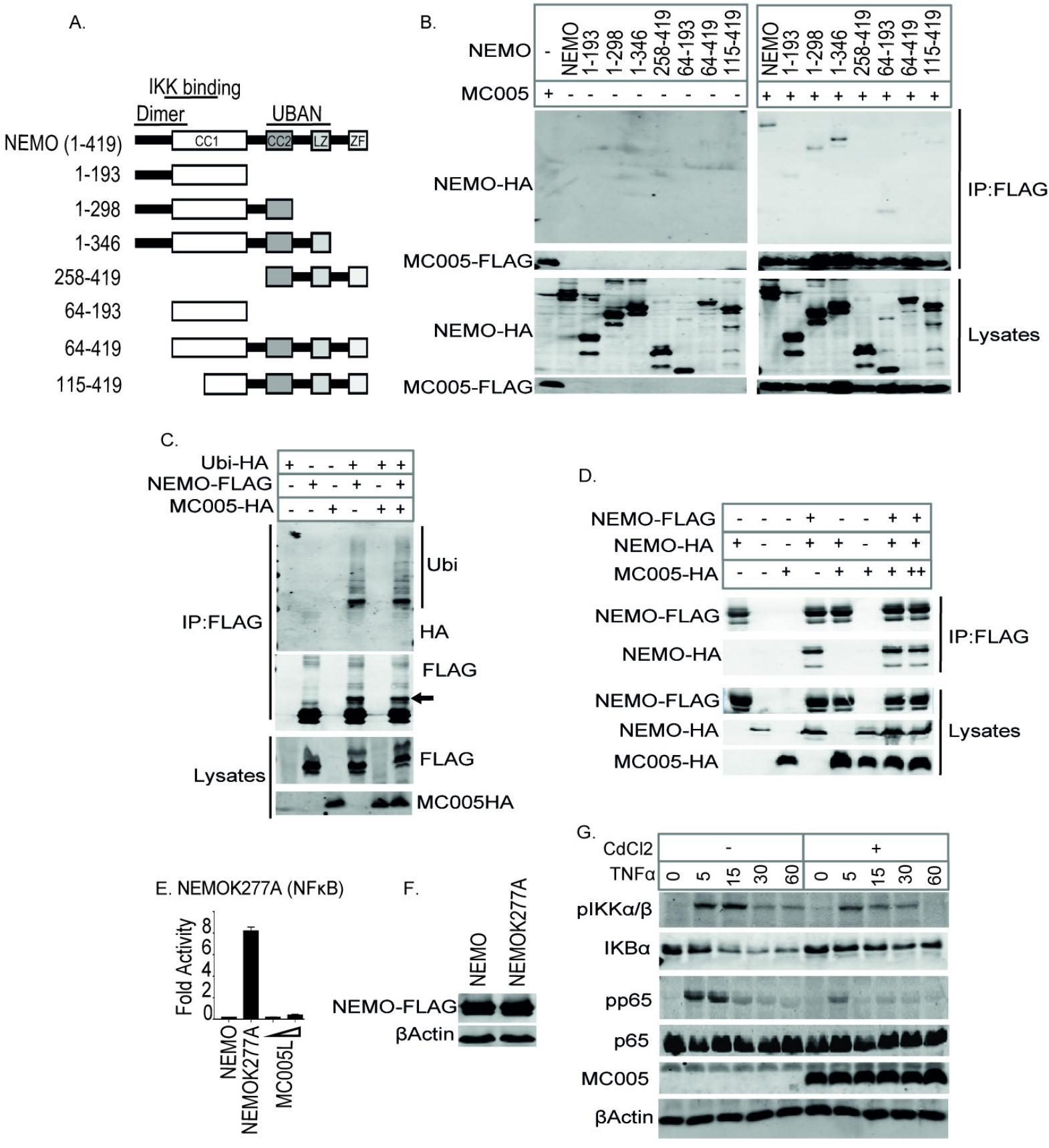
A.
IKK binding
Dimer
UBAN
NEMO (1-419)
CC1
CC2
LZ
ZF
1-193
1-298
1-346
258-419
64-193
64-419
115-419
B.
NEMO
MC005
NEMO
1-193
1-298
1-346
258-419
64-193
64-419
115-419
NEMO-HA
MC005-FLAG
IP:FLAG
Lysates
C.
Ubi-HA
NEMO-FLAG
MC005-HA
Ubi
IP:FLAG
HA
FLAG
Lysates
FLAG
MC005HA
D.
NEMO-FLAG
NEMO-HA
MC005-HA
IP:FLAG
Lysates
E. NEMOK277A (NFκB)
Fold Activity
NEMO
NEMOK277A
MC005L
F.
NEMO
NEMOK277A
NEMO-FLAG
βActin
G.
CdCl2
TNFα
pIKKα/β
IKBα
pp65
p65
MC005
βActin

Figure 8.

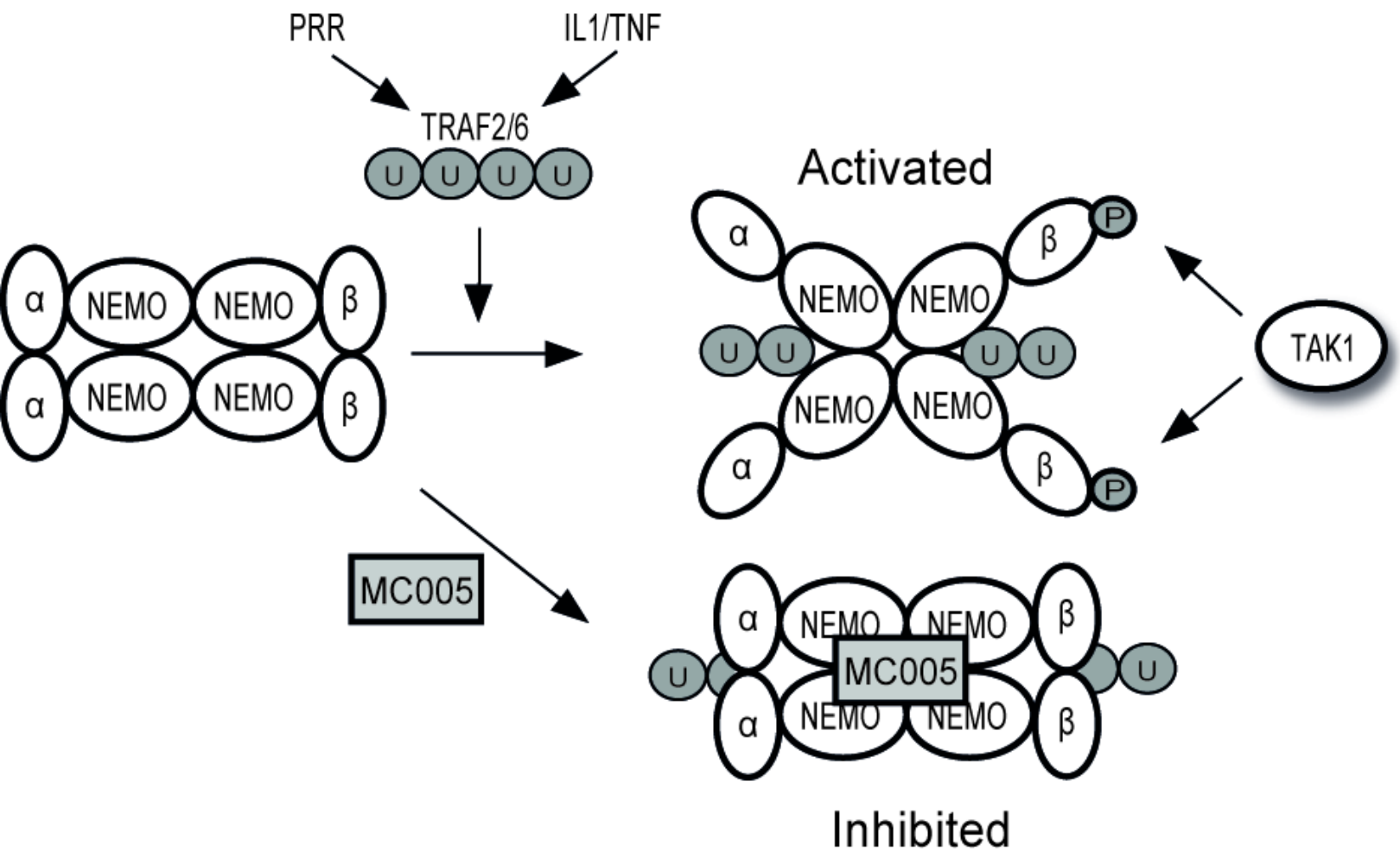
PRR
IL1/TNF
TRAF2/6
U U U U
α
NEMO
NEMO
β
α
NEMO
NEMO
β
Activated
α
β
P
NEMO
NEMO
U U
U U
NEMO
NEMO
α
β
P
TAK1
MC005
α
NEMO
NEMO
β
U
MC005
U
α
NEMO
NEMO
β
Inhibited